A COMPARISON OF TWO CO-BASED METHODS FOR QUANTIFYING ANTHROPOGENIC CO_2 SOURCES AT REGIONAL SCALES

LU, L. J.[1,2] – LI, B.[1*]

[1]*College of Resource and Environment, Anhui Science and Technology University, Bengbu 233000, China*

[2]*Key Laboratory of Digital Rural Construction and Governance, Anhui Provincial Department of Science and Technology, Bengbu 233000, China*

**Corresponding author*
e-mail: boli_ahstu@163.com

(Received 16th Apr 2024; accepted 8th Jul 2024)

Abstract. Two CO-based methods either using the atmospheric CO_2/CO ratio or the combustion CO_2/CO ratio, were used to invert the anthropogenic CO_2 emission flux in two distinct areas of China: Waliguan (WLG, CO_2 dominated by mixed biogenic and anthropogenic emissions) and Shangdianzi (SDZ, CO_2 dominated by anthropogenic emissions). A flux inversion system was conducted by incorporating the POD4DVAR method with the Community Multiscale Air Quality (CMAQ) model, and the system was then applied to the two areas using 2016 data for CO_2 flux inversions based on the two ratios of CO_2/CO. Results show that both a posteriori CO_2 fluxes are overall higher than the a priori flux, which indicates a systematic underestimation of the a priori data in both areas. A comparison of the observations and simulations shows that a posteriori estimates based on combustion ratio of CO_2/CO can greatly improve the agreement between observed and modeled concentrations, especially in areas where the variation of atmosphere CO_2 concentration is larger, such as in SDZ. Though the model accuracy using the ratio of atmospheric CO_2/CO was improved, the difference between simulations and observations is still large. the inversion based on the combustion CO_2/CO ratios has better results for regional CO_2 flux inversion. Based on this method with combination of validated a priori and in situ CO continuous observations, we can obtain anthropogenic CO_2 emission estimation with high accuracy.
Keywords: *anthropogenic, CO, POD4DVAR, CMAQ, flux inversion*

Introduction

Global warming, which is caused by excess greenhouse gases in the atmosphere, has attracted increasing attention in recent years. The greenhouse gases, especially CO_2, are generally considered to be greatly influenced by anthropogenic emissions. Even in some rural areas far from cities, over 30% of the atmospheric CO_2 comes from burning fossil fuels (i.e., petrol, coal, and natural gas) (Levin and Karstens, 2008). It is very important to separate anthropogenic sources from the total CO_2 sources in the atmosphere, which can help us understand spatial-temporal variations on the Earth's surface. In CO_2 cycle process, fossil fuel burning and biospheric respiration are the two main sources, while photosynthesis can absorb some CO_2. However, these sources and sinks are not isolated in their distribution but are instead overlapped in many regions in the world. (Hu et al., 2018; Yue et al., 2016). It is difficult to clearly separate these sources and sinks in inversion models without enough information (Levin and Karstens, 2007).

The anthropogenic contribution to the atmospheric CO_2 signature can be investigated using "bottom-up" approach (Feng et al., 2017; Li et al., 2015) and it is labor-intensive and time-consuming, anthropogenic emissions inventories based on "bottom-up" approach always have underlying uncertainties and require careful validation when used in realistic applications (Ohara et al., 2007; Sahu et al., 2015). Based on these a priori emission inventories and observations, atmospheric transport models and some mathematical algorithms are integrated to optimize inversion parameters and to obtain optimal flux (Zou et al., 2017; Gilliland, 2003). One shortcoming of inversion methods is that atmospheric CO_2 observations, generally, cannot guarantee spatial and temporal resolutions in realistic applications on regional scales. The Global Atmosphere Watch (GAW) program of the World Meteorological Organization (WMO) has nearly 200 observation sites providing continuous CO_2 measurements with only 4 located in China that provide completely unsatisfactory data based on CO_2 flux inversion, especially on regional scales (Fang et al., 2017).

To solve this problem, additional information on auxiliary tracers has been taken into account for inversion, among which radiocarbon measurements of atmospheric CO_2 has been an excellent tracer for fossil fuel CO_2 on regional, continental, and global scales (Turnbull et al., 2006; Levin et al., 2003; Levin and Hesshaimer, 2000; Svetlik et al., 2010). However, long-term, high precision $^{14}CO_2$ monitoring is too laborious and expensive to be carried out in practice. (Levin and Kromer, 2004; Meijer et al., 1996).

Other tracers for anthropogenic CO_2 have also been used in some studies, e.g., CFCs, C_2H_2, SF_6 and, especially, carbon monoxide (CO) (Turnbull et al., 2006; Rivier et al., 2006; Bakwin et al., 1997). Generally, a good tracer must have the following three characteristics: (1) it should have a good relativity with CO_2, (2) it should be easy to continuously measure, and (3) its behavior should be well understood with a relatively clear chemical mechanism (Djuricin et al., 2010). CFCs and SF_6 are relatively stable in the troposphere, but their biggest drawbacks in use of the inversion process is that they are not directly linked to fossil fuel CO_2. In contrast, CO is a concomitant product of CO_2 in combustion processes, and it can be easily obtained at air quality monitoring sites (Gamnitzer et al., 2006; Potosnak et al., 1999). One challenge, however, is that CO_2/CO ratios largely depend on both the source and the combustion efficiency, which has significant uncertainties for various fossil fuel sources (Vogel et al., 2017; Suntharalingam et al., 2004). CO has a lifetime of approximately two months, and it easily reacts with other substances in the atmosphere, so realistic applications should take these characteristics into consideration. On the other hand, CO_2/CO emission ratios vary in different fossil fuel sources and regions, necessitating detailed investigation and careful validation when using inversion models (Palmer et al., 2006).

In order to obtain more accurate posteriors and their simulations, a flux inversion system was constructed by incorporating the POD4DVAR method into the CMAQ model, and the system was then applied to two distinct areas of China, i.e., SDZ and WLG, for inversion of CO_2 fluxes based on two kinds of CO mixing ratios. WLG is located in the middle-west region of China with a relatively underdeveloped industrial foundation, and a large portion of atmospheric CO_2 is affected by biogenic activities. In contrast, SDZ lies in the Jing-Jin-Tang area, one of the most industrialized regions of China, and its atmospheric CO_2 is dominated by anthropogenic activities such as burning fossil fuels (i.e., petrol, coal, and natural gas). We first investigate specific contributions of each source with experiments using the CMAQ model, and natural sources of CO are neglected because they represent a very small contribution to total CO in the two locations. Second, two CO_2/CO ratios (i.e., R_{atm}: atmospheric CO_2/CO and R_{com}: combustion CO_2/CO) were used in our inversion system for a posteriori anthropogenic CO_2 fluxes. Then, a comparison with the MIX inventory a priori and the

http://www.aloki.hu ● ISSN 1589 1623 (Print) ● ISSN 1785 0037 (Online)
DOI: http://dx.doi.org/10.15666/aeer/2206_53115327

two a posteriori fluxes was conducted. Lastly, we compared simulations based on the two a posteriori inversion fluxes and satellite observations for a detailed analysis of the a posteriori uncertainty. The measurements of CO and CO_2 are shown in the section "Models and data," and the two CO-based methods are illustrated in the section "CO-based methods for quantifying anthropogenic CO_2." The section "Results and discussion" shows the results of the two CO-based inversion methods, and a comparison and detailed discussion is also conducted in this section. The section "Conclusion" summarizes the conclusions.

Models and data

Study areas

China has a vast land area covering approximately 9,600,000 km^2 with unbalanced development in different regions, which leads to a great difference in anthropogenic CO_2 emissions between the west and east of the country. The two distinct areas, i.e., SDZ and WLG (*Fig. 1*), to some extent, represent two kinds of regions with different characteristics of greenhouse gas emissions. SDZ, located on the North China Plain, covers the region of Jing-Jin-Tang, which is one of the highest urbanized regions. The total population is over 60 million in this area, emitting a large amount of CO_2 with daily activities. There is one Global Atmosphere Watch (GAW) station, i.e., SDZ, in this area, which lies northeast of Beijing city, with low population and industrial density and, thus, the CO_2 concentration is dominated by natural sources. WLG, unlike SDZ, is located in a region with a relatively underdeveloped industrial foundation, covering parts of Qinghai and Gansu provinces. In this area, atmospheric CO_2 is influenced simultaneously by anthropogenic and natural emissions. The purpose of choosing these two areas is to investigate the characteristics of emission mechanisms and uncertainties in CO-based inversion methods for CO_2 flux in different areas.

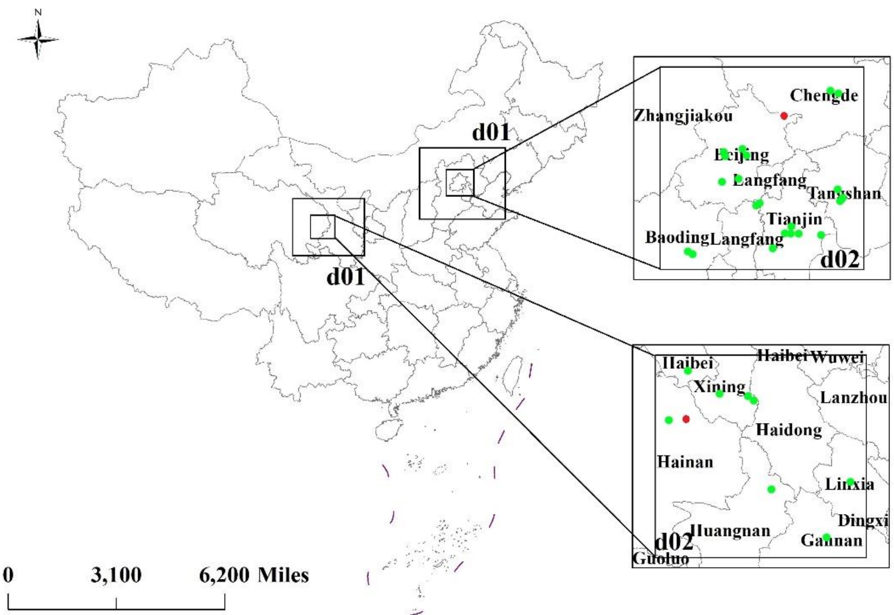

Figure 1. *The two study areas: d02 is our inner area and d02 is the boundary layer area for providing boundary fields for d01. The green dots are the CO monitoring sites used in this paper, the red dots are the GAW monitoring sites in WLG and SDZ respectively*

http://www.aloki.hu ● ISSN 1589 1623 (Print) ● ISSN 1785 0037 (Online)
DOI: http://dx.doi.org/10.15666/aeer/2206_53115327

CO and CO_2 measurements

Hourly averaged CO mixing ratios in 2016 from the air quality network of The Ministry of Environment Protection of the People's Republic (http://106.37.208.233:20035/) were collected for inversion. This monitoring network consists of 496 stations including 74 cities in China. CO, along with six other air pollutants, was monitored at hourly time steps. In situ CO observations from 22 monitoring sites in SDZ and 9 monitoring sites in WLG were collected for the next step. In our study, CO measurements are mainly used for two thresholds:

(1) Get the pseudo-CO_2 observations based on atmospheric CO_2/CO ratios.

(2) Get the optimal CO emission inventory based on in situ CO observations. Details about this will be illustrated later.

CO_2 measurements in our study mainly come from satellite observations, i.e., GOSAT and OCO-2. The temporal resolution of satellite observations is limited by the transit frequency, so the satellite observations are discontinuous in time such that only time-compliant observations are collected and applied to our analysis. Before the CO_2 measurements are used in realistic applications, the raw data have been filtered to remove outlier values (over $\pm 3\sigma$) at all time points. In this paper, our CO_2 measurements are only used for validation for inversion results by the two CO-based methods.

Emission inventories

The a priori fluxes of CO and CO_2 from anthropogenic activities were extracted from the MIX inventory of Multi-resolution Emission Inventory for China (MEIC, http://www.meicmodel.org/index.html) at Tsinghua University. The emission inventory includes all major anthropogenic sources in Asia in 2010, including NO_x, SO_2, NH_3, CO, NMVOC, $PM_{2.5}$, PM_{10}, OC, BC, CO_2, and others. The resolution of this inventory is 0.25 degrees with emissions from five sectors, i.e., industry, power, residential, agriculture and transport (Li et al., 2017). In our study, emission inventories were used for providing CO_2/CO correlations in the inversion system.

Natural sources of CO_2 were extracted from the Terra/MODIS Gross Primary Productivity (GPP) product (MOD17A2H), which is a Level 4 gridded product with sinusoidal projection, and it is an 8-day composite having 500 m spatial resolution in both longitude and latitude. Our natural source of CO_2 was derived from the PsnNet_500m field in the MOD17A2H product.

Model description

In our study, we used a 3D transport model, CMAQ, for CO_2 simulations, which were then simultaneously used for flux inversion and comparison with observations. Generally, CO_2 simulations were not supported in the original CMAQ model, so before running our inversion system, we added the new species "CO_2" to the code of the CMAQ model. In this paper, CMAQ was run with a Lambert conformal projection and a two-nested grid configuration in the two study areas, i.e., d01, d02. The horizontal resolution of d01 is 3 km and encompasses a few cities measuring 174 × 410 km and 190 × 341 km around SDZ and WLG, respectively, as shown in *Figure 1*. The computations were made on 22 vertical levels. The underlying surface data in the model, e.g., landcover, soil type, digital elevation and other characteristics, were all derived from WRF's default geographical data. The d02 domain covers areas measuring

http://www.aloki.hu ● ISSN 1589 1623 (Print) ● ISSN 1785 0037 (Online)
DOI: http://dx.doi.org/10.15666/aeer/2206_53115327

442 × 1080 km and 436 × 841 km in SDZ and WLG, respectively, with a resolution of 9 km. The main purpose of the d02 nest is to provide lateral and initial boundary fields for the d01 domain. CMAQ was run in “spin-up” with the a priori MIX emissions, and the results were used for the initial fields in every assimilation time window. The configurations mentioned above were adopted in all simulation processes with the a priori MIX dataset and the two a posteriori inversion fluxes.

A flux inversion system was constructed by incorporating the POD4DVAR method into the CMAQ model. This system can be simultaneously used for flux inversion on CO and CO_2, and details about the system can be seen in prior studies (Lu et al., 2019). In our current study, the system is used for two thresholds: (1) flux inversion of CO with the CO observations and then CO_2 flux obtained with the R_{com} and CO flux and (2) the inversion of CO_2 with the pseudo-CO_2 observations.

CO-based methods for quantifying anthropogenic CO_2

CO_2/CO ratios

Generally, observations play an important role in an inversion system; insufficient CO_2, whether in situ or from satellite observations, greatly restricts the application of CO_2 emission inversion, especially on a regional scale. In contrast, abundant CO observations can be collected from the air quality monitoring network of The Ministry of Environment Protection of the People’s Republic of China which has over 5000 observation sites around the country. In our two study areas, we have continuously collected CO measurements from 31 observation stations, providing much more data than are available either in situ or from satellite CO_2 observations. A natural way is to generate atmospheric CO_2 from in situ CO observations based on the atmospheric CO_2/CO ratios. Generally, there are two CO_2/CO ratios we can used for anthropogenic CO_2 emission inversion: atmospheric CO_2/CO ratios (R_{atm}) and combustion CO_2/CO ratios (R_{com}) in emission inventories such as the MIX.

CO and CO_2, generally, exist simultaneously in the atmosphere with a relatively stable ratio for a specific time and area. In our study, the first kind of CO_2/CO ratio, i.e., R_{atm}, was extracted from in situ CO and CO_2 measurements from the SDZ and WLG monitoring stations as follows (Gamnitzer et al., 2006):

(1) Extract CO_2 and CO observations from the SDZ and WLG monitoring stations (the dataset can be downloaded from the World Data Centre for Greenhous Gases https://gaw.kishou.go.jp/).

(2) Get the ΔCO and ΔCO_2 from $\Delta CO = CO_{obs} - CO_{bg}$ and $\Delta CO_2 = CO_{obs} - CO_{2bg}$, where obs is observations of CO and CO_2 extracted from the SDZ and WLG monitoring stations, respectively, and CO_{bg} and CO_{2bg} are the backgrounds of CO and CO_2, respectively.

(3) Generate R_{atm} ($\Delta CO/\Delta CO_2$).

The second kind of CO_2/CO ratio, i.e., R_{com}, was derived from the MIX emissions inventory. As mentioned in the section “Emission inventories,” the a priori MIX dataset includes total anthropogenic CO_2 and CO emissions, from which combustion CO_2/CO ratios can be derived. After the two kinds of CO2/CO ratios were collected, the two CO-based CO2 emission inversion methods can be illustrated as described in the sections “Calculating anthropogenic CO2 emissions based on combustion CO/CO2 ratios” and “Calculating anthropogenic CO2 emissions based on atmospheric ΔCO/ΔCO2 ratios,” respectively.

http://www.aloki.hu ● ISSN 1589 1623 (Print) ● ISSN 1785 0037 (Online)
DOI: http://dx.doi.org/10.15666/aeer/2206_53115327

Calculating anthropogenic CO_2 emissions based on combustion CO/CO_2 ratios

With the combustion CO/CO_2 ratios and an optimal CO emissions flux, the hourly anthropogenic CO_2 emission flux can be inversed as illustrated in the following procedure (Zhao et al., 2024):

(1) Extracting combustion CO_2/CO ratios from the a priori MIX dataset. The MIX covers the whole country of China, from which two smaller-area a priori values for our two study areas were extracted. The two a priori grids contain the same rows and columns as described in the section "Model description," and the combustion ratios (R_{com}) were calculated based on the values of CO_2 and CO in the two extracted emission inventories (Shan et al., 2023; Mottungan et al., 2024).

(2) Deriving an optimal anthropogenic CO emission flux. Hourly in situ CO observations in the two study areas were collected and were then applied to our inversion system for an optimal anthropogenic CO emission flux.

(3) Calculating the optimal anthropogenic CO_2 emission flux. With the optimal anthropogenic CO emission flux and R_{com}, we can get the optimal anthropogenic CO_2 flux by multiplying CO(o) by R_{com} as illustrated below (*Eq. 1*):

$$CO_{2\text{-com}} = CO_o \times R_{com} \tag{Eq.1}$$

where $CO_{2\text{-com}}$ indicates whether the anthropogenic CO_2 emissions are the same as those in the first method, CO_o represents the optimal inversion of CO flux based on the continuous CO in situ measurements, and R_{com} is the gridded CO_2/CO ratios from the a priori MIX dataset.

Calculating anthropogenic CO_2 emissions based on atmospheric $\Delta CO/\Delta CO_2$ ratios

With the R_{atm} and in situ CO observations, hourly anthropogenic CO_2 emission flux can be derived as illustrated in the following procedure:

(1) Deriving hourly pseudo-surface CO_2 observations. With the R_{atm} calculated above and in situ CO observations, we can get the CO_2 observations, namely, pseudo-surface CO_2, from multiple CO observations by R_{atm} because they are not real observations.

(2) Applying hourly pseudo-surface CO_2 observations into our inversion system for optimal total CO_2 flux ($POST_a$).

(3) Calculating the anthropogenic CO_2 emissions, $CO_{2\text{-a}}$, with $POST_a$ and $CO_{2\text{-n}}$. There are mainly two sources of CO_2, i.e., anthropogenic and natural; with the $POST_a$ and $Flux_n$, the anthropogenic CO_2 sources can be calculated according to the following formula (*Eq. 2*):

$$CO_{2\text{-atm}} = POST_a - CO_{2\text{-n}} \tag{Eq.2}$$

where $CO_{2\text{-atm}}$ represents anthropogenic CO_2 emissions, $POST_a$ is the optimal inversion of total CO_2 flux from R_{atm}-based CO_2 atmospheric pseudo-observations, and $CO_{2\text{-n}}$ are the natural CO_2 emissions.

Results and discussion

R_{com} and R_{atm}

As mentioned above, R_{com} is used for CO_2 flux inversion in the R_{com}-based inversion method (section "Calculating anthropogenic CO2 emissions based on

http://www.aloki.hu ● ISSN 1589 1623 (Print) ● ISSN 1785 0037 (Online)
DOI: http://dx.doi.org/10.15666/aeer/2206_53115327

combustion CO/CO2 ratios”). The R_{com} used in this paper is mainly extracted from the a priori MIX dataset released by the MEIC team. We first extracted CO_2 and CO fluxes over our two study areas and then generated the R_{com}. Results (*Figs. 2* and *3*) show that R_{com} in most areas of SDZ is between 10 and 40 (85%), and the overall average is 27.89. The maximum proportion is 184.1 (*Table 1*) and is located in the southeast of the study area in July. This area is near the sea, which has very low CO emissions, leading to the high proportions in this area. The minimum R_{com} is 10.13 and appears in the northwest of the study area in January and February. This area has a relatively small population and lower city densities, which also indicates that there is a lower combustion efficiency in the rural areas where more CO would be produced under the same conditions compared to other areas. From a seasonal perspective, R_{com} in the summer and autumn is significantly higher, approximately 1.3 times, than in the spring and winter. Large values of R_{com} are mainly located in urban areas and their annexes, especially in Beijing-Tianjin-Tangshan, which is one of the most developed industrial areas in China.

Table 1. *R_{com} of the a priori in SDZ and WLG*

Time		Jan	Feb	Mar	Apr	May	Jun	Jul	Aug	Sep	Oct	Nov	Dec
SDZ	Min	10.13	10.13	12.04	15.03	15.14	15.85	15.33	15.21	15.47	15.24	11.66	10.89
	Max	84.09	84.09	109.4	121.3	166.5	171.1	184.1	184.0	167.6	161.6	154.8	139.8
	Mean	19.34	19.27	24.13	26.59	28.59	31.84	32.53	31.24	33.37	31.38	29.01	27.3
WLG	Min	8.95	9.07	9.49	11.17	13.13	13.56	13.44	13.48	13.59	11.28	9.4	9.13
	Max	158.8	160.3	178.4	197.7	195.2	189.4	200.4	153.5	194.0	195.4	134.4	128.0
	Mean	19.25	19.75	22.21	29.01	32	32.22	32.64	30.29	32.69	29.72	21.04	19.37

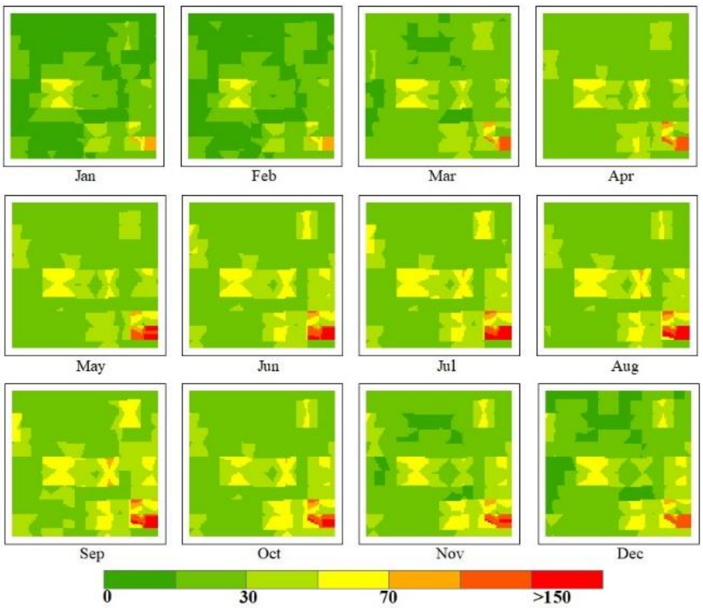

Figure 2. *CO_2/CO correlations from MIX in SDZ*

In WLG, the majority of the R_{com} values are between 8.95 and 24 (80%), and the overall mean value is 26.68, which is not significantly different from that of SDZ. The

http://www.aloki.hu ● ISSN 1589 1623 (Print) ● ISSN 1785 0037 (Online)
DOI: http://dx.doi.org/10.15666/aeer/2206_53115327

maximum R_{com} is 200.39, mainly in the northern part of the study area. This area has the highest population and the most cities and industries. The minimum R_{com} is 8.95 and appears in the southern part of the study area. This area has a lower population and better vegetation coverage. Like in SDZ, R_{com} in WLG also tends towards significant seasonal variation, i.e., R_{com} is higher in the summer and autumn than in the spring and winter. R_{com} in the summer and autumn is approximately 23.6 and is approximately 29.8 in the spring and winter.

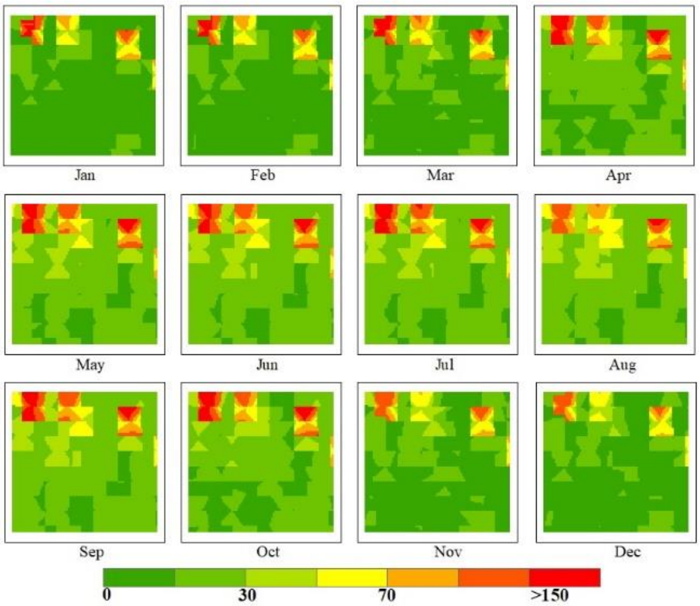

Figure 3. *CO_2/CO correlations from MIX in WLG*

In summary, whether in SDZ or WLG, the highest CO_2/CO ratios generally occur in either the summer or autumn. During these periods, the proportion of CO_2 to CO has increased significantly due to both the reduction of CO produced by residential heating and fossil fuel burning and the decomposition of some of the CO at high temperatures. At the same time, the high proportions of CO_2 to CO are mainly distributed in urban areas and suburbs. Because of improvements in industrial technology, insufficient combustion in urban areas is much less than in rural areas under the same conditions, which leads to a significant reduction in the total amount of CO, thus providing high proportions of CO_2 to CO.

In this paper, R_{atm} is mainly derived from ground-based CO_2 and CO observations. There are two atmospheric background stations in our two study areas, i.e., SDZ and WLG. Although concentrations of CO_2 and CO are affected by many factors, e.g., meteorological field and emission intensity, it is assumed that R_{atm} is relatively stable in a specific area over a short period. In this paper, there is a fixed R_{atm} in each month, and every fixed R_{atm} is derived from CO_2 and CO observations from the SDZ and WLG sites. Details of obtaining R_{atm} are illustrated in the section "CO2/CO ratios," and the results are shown in *Table 2*.

In SDZ, the maximum R_{atm} is 62.22 in May, the minimum is 39.18 in July, and the average over the whole year is 52.17. In WLG, the maximum R_{atm} is 59.51 in December, the minimum is 22 in April, and the average over the whole year is 39.21,

http://www.aloki.hu ● ISSN 1589 1623 (Print) ● ISSN 1785 0037 (Online)
DOI: http://dx.doi.org/10.15666/aeer/2206_53115327

which is much lower than the average R_{atm} in SDZ. Results also show that R_{atm} in SDZ and WLG have similar variation tendencies at most time points, except in spring. SDZ has the highest R_{atm} in spring, while WLG has the lowest R_{atm} in spring.

Table 2. *R_{atm} in SDZ and WLG. R_{atm} are the atmospheric CO_2/CO ratios*

Time	Mar	Apr	May	Jun	Jul	Aug	Sep	Oct	Nov	Dec	Jan	Feb
SDZ	56.98	50.2	62.22	53.9	39.18	44.48	59.18	42.06	49.94	57.1	45.25	50.6
	Spring: 56.47			Summer: 45.85			Autumn: 50.39			Winter: 50.98		
WLG	32.79	22	28.01	38.56	34.01	37.7	36.15	42.5	52.65	59.51	42.74	43.86
	Spring: 27.6			Summer: 36.76			Autumn: 43.77			Winter: 48.7		

Oxidation sources of CO

Tropospheric CO is mainly from incomplete combustion, and a small part originates from the oxidation of hydrocarbons. CO has an important influence on atmospheric chemistry because of its significant removal of OH which then affects production and depletion of other substances. It has an atmospheric lifetime of approximately two months against oxidation by the OH radical. However, the amount of CO removed by OH is not clear and varies in different places and atmospheric conditions, factors that should be investigated in detail before using the inversion process for a specific area. Before using CO for anthropogenic CO_2 emission inversion, we first conduct experiments to investigate what percentage of CO is caused by oxidation processes.

Within CMAQ, CO mainly comes from several secondary photochemical routes with other species, e.g., CH_4, FORM, ALDX, ALD_2, OLE, IOLE, OPEN, ETH, ISOP and ISOD. These species can directly generate CO by reacting with either O, O_3 or OH. In the oxidation experiments, simulations are performed for two days every week in 2016. The effects of these species are evaluated here by a priori emissions, initial conditions (ICs) and boundary conditions (BCs) for every species. The value of each species is set to zero for each run, and the results are averaged every week.

Experimental results (*Fig. 4*) show that the number of CO oxidation sources is small in both study areas. The average annual percentages of oxidation sources are 0.44% and 0.59% in SDZ and WLG (*Table 3*), respectively, indicating that these sources have little effect on the concentration of CO in the atmosphere. However, the sources of CO oxidation in the two regions are obviously different in the winter compared to the summer, i.e., there are obvious oxidation reactions in the summer and almost no oxidation occurs in winter. The sources of CO oxidation in the summer are approximately five times greater than those in winter. The main reason for this phenomenon is that the high temperature in summer greatly accelerates the reaction rate of CO oxidation with other species, such as OH, in the atmosphere. For all experimental periods, the percentage of oxidation in WLG is slightly higher than that in SDZ. However, the absolute amount of oxidation in SDZ is much larger than that in WLG because of its large amount of emissions. In the subsequent inversion process, the source of CO is used to obtain anthropogenic CO emissions, i.e., the total observed CO concentration minus the portion caused by oxidation. Anthropogenic CO emissions were then used for inversion of anthropogenic CO_2 flux in the two inversion methods.

http://www.aloki.hu ● ISSN 1589 1623 (Print) ● ISSN 1785 0037 (Online)
DOI: http://dx.doi.org/10.15666/aeer/2206_53115327

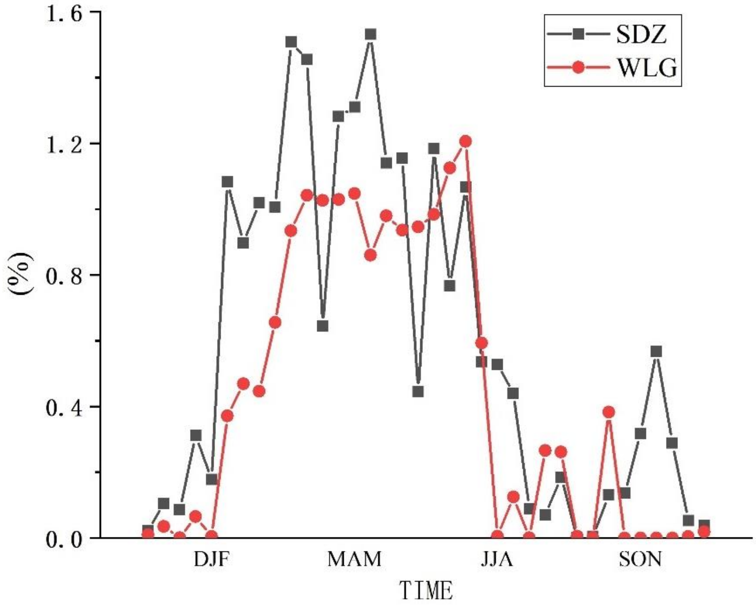

Figure 4. *Oxidation sources of CO in two study areas*

Table 3. *Percentages of oxidation sources of CO in the two study areas (%)*

	Min	Max	Mean
SDZ	0.00	1.21	0.44
WLG	0.00	1.53	0.59

Posteriors of anthropogenic CO_2 emissions

In our study, CO_2 emissions are considered to originate from two sources, natural and anthropogenic. The a priori MIX dataset was used to represent anthropogenic CO_2 emissions, and the natural source CO_2 comes from MODIS as mentioned in the section “Emission inventories.” The total emission is the sum of anthropogenic and natural source CO_2 which was used for realistic simulations in the CMAQ model. According to the two methods described in the section “CO-based methods for quantifying anthropogenic CO_2” and in situ hourly continuous CO observations, we obtained two anthropogenic CO_2 emission inventories, CO_2 (*atm*) and CO_2 (*com*), based on the ratios R_{com} and R_{atm}, respectively. By summing the two inventories and natural CO_2 sources, we got two a posteriori inventories, $POST_a$ and $POST_c$ (*Fig. 5*).

The inversion results show that the region of SDZ is a significant carbon source over all the simulated periods, with average emissions of 12.75, 17.92, and 19.3 moles/s in the a priori MIX, $POST_c$ and $POST_a$, respectively. In contrast, the WLG area is a significant carbon sink having average emissions of -3.46, -1.74, and -3.18 moles/s in the a priori MIX, $POST_c$ and $POST_a$, respectively.

As illustrated above, the natural source CO_2 was set to a constant value in all inversion processes, so we only discuss the anthropogenic CO_2 emissions here. Our inversion results show that anthropogenic emissions from the two a posteriori are generally higher than the a priori MIX values in both SDZ or WLG, and the a priori MIX dataset has significant underestimation during all periods of the year. Based on

http://www.aloki.hu ● ISSN 1589 1623 (Print) ● ISSN 1785 0037 (Online)
DOI: http://dx.doi.org/10.15666/aeer/2206_53115327

the R_{com} in SDZ, the percentage increases are 28.5%, 31.8%, 27.1%, and 28.9% in the spring, summer, autumn and winter, respectively, with an average of 29.1% representing the annual growth rate. In WLG, the total emissions increase is 116.5%, and quarterly growth rates become 113.7%, 114%, 115.3%, and 123% in the spring, summer, autumn and winter, respectively. Based on the R_{atm} in SDZ, the total growth is 35.3% and seasonal growth is 20.2%, 25.1%, 32.2%, and 63.7% in the spring, summer, autumn and winter, respectively. In WLG, anthropogenic emissions increased by 18.9% in total compared with the a priori MIX dataset, and seasonal growth was 25.5%, 9.5%, 23%, and 17.4% in the spring, summer, autumn and winter, respectively (*Table 4*).

Comparison of simulations and observations

In this section, CMAQ simulations based on the a priori MIX dataset, $POST_a$, and $POST_c$ were compared to satellite observations of GOSAT and OCO2 (*Fig. 6*). Because of the importance of the initial field and the boundary layer, a one-month, i.e., from December 1st to December 31st in 2015, “spin-up” was conducted to prove proper initial constraints for CMAQ. The boundary layer for simulations was extracted from CarbonTracker (CT), which is generated and managed by The NOAA Earth System Research Laboratory.

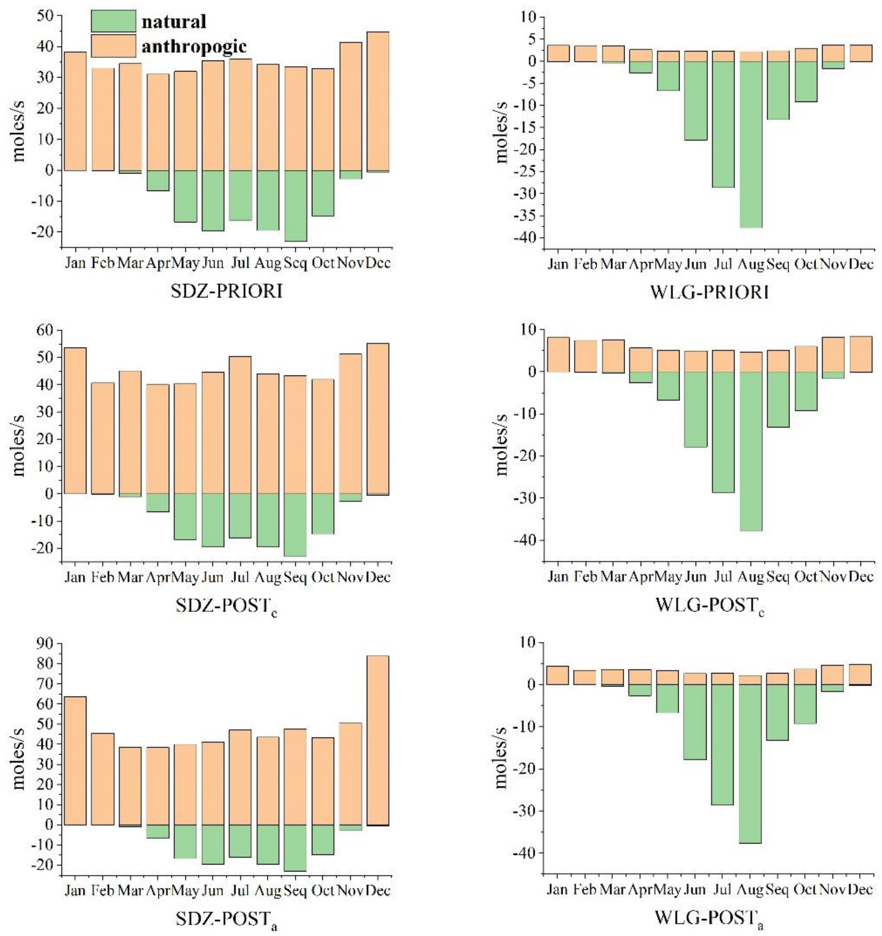

Figure 5. *Monthly CO_2 emissions from the a priori MIX dataset, $POST_a$ and $POST_c$. $POST_a$ and $POST_c$ are a posteriori inversion fluxes based on the R_{atm} and R_{com} method, respectively*

http://www.aloki.hu ● ISSN 1589 1623 (Print) ● ISSN 1785 0037 (Online)
DOI: http://dx.doi.org/10.15666/aeer/2206_53115327

***Table 4.** The growth rates of $POST_c$ and $POST_a$ in the two study areas (%)*

	SDZ												
	Dec	**Jan**	**Feb**	**Mar**	**Apr**	**May**	**Jun**	**Jul**	**Aug**	**Sep**	**Oct**	**Nov**	**Avg**
$POST_c$	23.4	40.2	23.2	30.7	28.6	26.2	26.0	40.5	28.8	29.6	27.7	24.1	29.1
	DJF: 28.9			MAM: 28.5			JJA: 31.8			SON: 27.1			
$POST_a$	87.3	66.1	37.6	11.7	23.5	25.3	16.4	31.4	27.5	42.6	31.7	22.2	35.3
	DJF: 63.7			MAM: 20.2			JJA:25.1			SON: 32.2			
	WLG												
	Dec	Jan	Feb	Mar	Apr	May	Jun	Jul	Aug	Sep	Oct	Nov	Avg
$POST_c$	128	124	117	116	113	112	114	114	114	113	111	122	116.5
	DJF: 123			MAM: 113.7			JJA: 114			SON: 115.3			
$POST_a$	30	22.6	-0.3	2.7	34.5	39.3	14.2	12.8	1.6	13.2	29.7	26.2	18.9
	DJF: 17.4			MAM: 25.5			JJA:9.5			SON: 23			

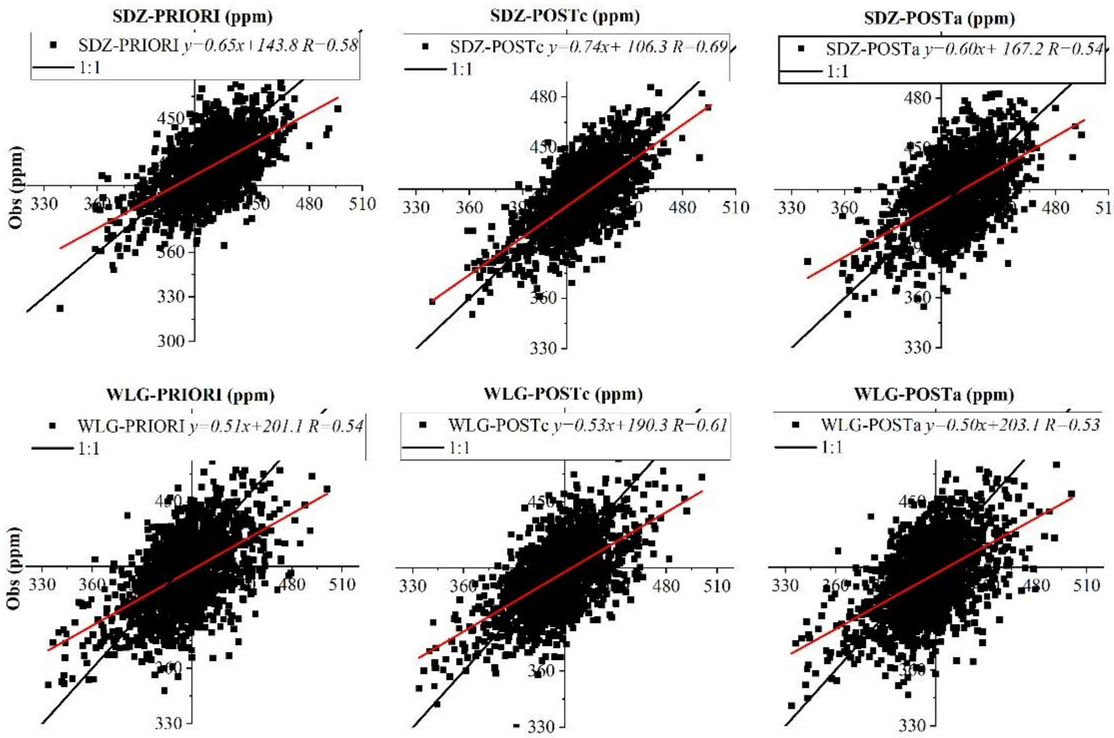

***Figure 6.** CO_2 observations and simulations from the a priori MIX dataset, and the $POST_a$ and the $POST_c$, respectively*

The results show that simulations based on the a priori MIX dataset can grasp the basic trend of CO_2 concentration variation in both SDZ and WLG, and correlation *r* values are 0.58 and 0.54 in SDZ and WLG, respectively. From a yearlong perspective, the simulations have a significant underestimation compared to observations in both areas, i.e., 6.40 ppm and 6.46 ppm in SDZ and WLG, respectively. In summary, a comprehensive underestimation occurred in the simulations based on the a priori MIX dataset in both study areas but especially in SDZ, which means there are significant uncertainties in using the a priori MIX dataset.

http://www.aloki.hu ● ISSN 1589 1623 (Print) ● ISSN 1785 0037 (Online)
DOI: http://dx.doi.org/10.15666/aeer/2206_53115327

Compared with the a priori MIX dataset, $POST_a$-based simulations performed poorly in both study areas. In SDZ, simulation accuracy by $POST_a$ showed great improvement in modeled errors, i.e., E_{mean} ranged from 6.40 ppm to 0.72 ppm, which was mainly due to the substantial increase in total flux from $POST_a$. However, the correlation r values between observations and simulations declined slightly, i.e., r ranged from 0.58 to 0.54 in SDZ and from 0.54 to 0.53 in WLG. This means that the increased values in $POST_a$ cannot reflect actual spatial-temporal variations in CO_2 flux. In WLG, $POST_a$-based simulations also performed poorly; E_{mean} has no significant improvement over all the simulated periods, i.e., 6.46 ppm to 6.11 ppm. This indicates that the atmospheric CO_2/CO-based inversion inventory still has significant uncertainties. Correlation r values also show these simulation uncertainties, from 0.54 in the a priori MIX dataset to 0.53 in $POST_a$. Generally, CO concentrations may have obvious fluctuations over a specific period and location because of its active chemical activity. The derived pesudo-CO_2 inherit these CO instabilities, which leads to greater uncertainties in the CO_2 flux inversion.

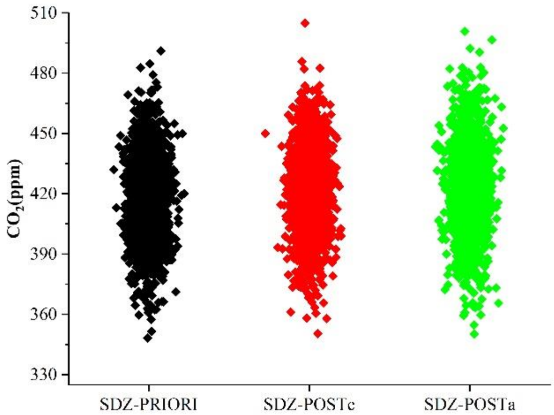

Compared with the simulations based on the a priori MIX dataset and $POST_a$, the accuracy of the simulations based on $POST_c$ has been improved significantly in both study areas but especially in some event periods in SDZ. E_{mean} values have become smaller than in the a priori MIX dataset, i.e., 2.28 ppm in SDZ and 5.12 ppm in WLG. The trend of CO_2 concentration variation can be grasped more accurately, i.e., correlation r values ranged from 0.58 to 0.69 in SDZ and from 0.54 to 0.61 in WLG (*Table 5; Fig. 6*), and the errors between the simulations and the observed values are also reduced significantly. This shows that $POST_c$ has better performance in reflecting the actual CO_2 emission intensity on the Earth's surface, which also illustrates the stability of the R_{com}-based method.

Table 5. *Errors and correlation, r, between observations and simulations (ppm)*

	SDZ			WLG		
	E_{mean}	E_{rmse}	r	E_{mean}	E_{rmse}	r
PRIORI	6.40	20.69	0.58	6.46	19.26	0.54
$POST_c$	2.28	20.47	0.69	5.12	18.16	0.61
$POST_a$	0.72	21.17	0.54	6.11	19.57	0.53

http://www.aloki.hu ● ISSN 1589 1623 (Print) ● ISSN 1785 0037 (Online)
DOI: http://dx.doi.org/10.15666/aeer/2206_53115327

Discussion

Active production and living activities in SDZ, which is one of the most developed industrial areas in China, contributed a large amount of CO_2 to the atmosphere. However, human activities in WLG are much weaker compared with those in SDZ. On the other hand, CO emissions in the two areas have obvious seasonal variations, i.e., emissions usually reach the highest levels in the winter and decrease slowly until the minimum level is reached in the summer. The main reason for this is that SDZ and WLG are located in northern China, where residential heating and related activities in the winter make significant contributions to the high levels of atmospheric CO_2 concentrations. The difference in WLG is that emission variations in the winter and summer are not obvious because of low intensity human activities in both the winter and summer. The variation patterns of natural source CO_2 exhibits the opposite trend compared to CO_2 from anthropogenic emissions, i.e., strong in the summer and weak in the winter, which mainly depends on the state of the local terrestrial ecosystem. In addition, regional natural CO_2 sources are greater in WLG than in SDZ, which led to the formation of a significant carbon sink in this area.

Overall, simulations based on $POST_c$ perform obviously better than those based on the a priori MIX dataset and $POST_a$. $POST_c$-based simulation accuracies and correlations show great improvement over all periods, especially in SDZ. Although an obvious improvement also appears (0.72 ppm of E_{mean} in SDZ) in $POST_a$-based simulations, significant errors still exist over the full year. In contrast, $POST_c$ can greatly reduce the errors in some pollution events, and simulations agree very well with observations. In addition, $POST_c$ simulations have lower dispersion than those of $POST_a$ and a priori MIX (*Fig. 7*), which indicates higher stability of the R_{com}-based method. In some cases, the R_{atm}-based method might improve the simulated accuracy, but there are still many uncertainties.

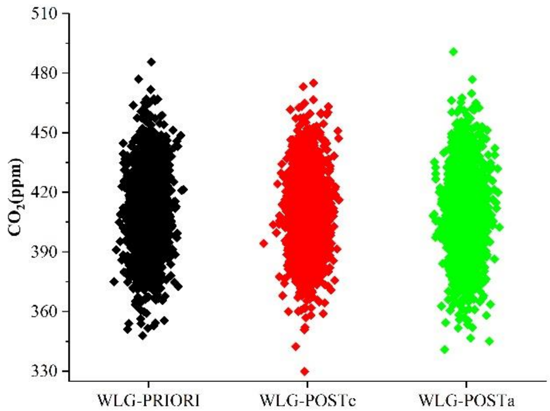

Figure 7. *Correlations of CO_2 observations and simulations. (a), (b), and (c) are correlations between CO_2 observations and simulations from the a priori MIX dataset, $POST_a$, and $POST_c$ in SDZ, respectively; (d), (e), and (f) are correlations between CO_2 observations and simulations from the a priori MIX dataset, $POST_a$, and $POST_c$, respectively, in WLG*

At a first glance, it seems that using CO measurements to quantify anthropogenic CO_2 emissions on a regional scale would introduce uncertainty. However, inversion results based on combustion CO_2/CO in our study show that using high temporal

http://www.aloki.hu ● ISSN 1589 1623 (Print) ● ISSN 1785 0037 (Online)
DOI: http://dx.doi.org/10.15666/aeer/2206_53115327

resolution CO observations as a quantitative tool for anthropogenic CO_2 emissions could significantly improve the agreement between observed and modeled concentrations, especially in areas where CO_2 concentration varies sharply, such as in SDZ. On the one hand, this shows the effectiveness of our inversion method based on CO_2/CO ratios, and on the other hand, it also demonstrates that ratios from the a priori MIX dataset can basically reflect the real situation of fuel burning. Compared with the R_{com}-based method, the inversion results based on atmospheric CO_2/CO ratios have significant uncertainties. Although the accuracy of the $POST_a$ simulation value has been improved over some periods, the simulation results are very uncertain during many times with large errors. This shows that the inversion results based on atmospheric CO_2/CO are not stable and are affected by the generation and consumption of CO in the atmosphere by different chemical reactions. On the other hand, the lack of continuous CO_2 observations cannot guarantee that there is enough atmospheric CO_2/CO ratio data for the inversion process. The atmospheric CO_2/CO ratios retrieved from inadequate sample observations lead directly to the huge uncertainty in the inversion inventory.

The inversion result shows that there is significant underestimation in the posterior fluxes compared to the priors, there are might two reasons: (1) the observed CO_2 concentration is lower than that on the earth surface, therefore the results obtained from the inversion based on this dataset will inevitably show a significant decrease; (2) The prior flux used in this article is obtained through traditional “bottom-up” methods, which are clearly influenced by artificial factors during the collecting procedure, ultimately bring significant uncertainties in the prior flux.

Conclusion

With the inversion system, regional CO_2 flux can be retrieved along with two CO_2/CO ratios from atmospheric and combustion sources and in situ CO continuous measurements, and then anthropogenic CO_2 emissions can be distinguished from the total flux. Simulations based on the two inverted fluxes show that the inversion results based on combustion CO_2/CO are stable and can significantly improve the simulation accuracy. The emission inventory based on atmospheric CO_2/CO inversion is affected by many factors and has great uncertainties. There are mainly two reasons for this: on the one hand, CO reacts with other substances during the process of atmospheric transport, and the concentration changes frequently; on the other hand, insufficient observations and statistical data are available to determine atmospheric CO_2/CO ratios on a regional scale, which greatly increases the uncertainty in atmospheric CO_2/CO ratios, affecting the accuracy of inversion emissions. Therefore, when using atmospheric CO_2/CO ratios to quantify CO_2 emissions, we should take a cautious attitude and put this method into practice only after full analysis. Although there are some abnormal proportions in combustion CO_2/CO ratios, after eliminating the abnormal data, the proportionality data can reflect the basic proportionality relationship in the region. Based on this proportionality data, a more accurate carbon dioxide emission inventory can be retrieved. Combustion CO_2/CO ratios are an appropriate proxy to estimate regional anthropogenic CO_2 emissions and then obtain total CO_2 emissions combined with natural sources of CO_2 from the MOD17A2H product.

Acknowledgments. This research was financially supported by an international partnership program of Chinese Academy of Sciences (Grant #131A11KYSB20170025), research grants from the National Key

R&D Program of China (2018YFA0606001, 2017YFA0604301, 2017YFA0604302, 2017YFC0503904), a research project funded by the State Key Laboratory of Resources and Environmental Information System (O88RA901YA, O8R8A085YA), a project funded by the National Natural Science Foundation of China (41771114) and Research Project of Anhui Provincial Department of Education (2023AH051878, 2023AH040280).

REFERENCES

[1] Bakwin, S., Hurst, D. F., Tans, P. P., Elkins, J. W. (1997): Anthropogenic sources of halocarbons, sulfur hexafluoride, carbon monoxide, and methane in the southeastern United States. – Journal of Geophysical Research Atmospheres 102: 15915-15925.

[2] Djuricin, S., Pataki, D. E., Xu, X. (2010): A comparison of tracer methods for quantifying CO_2 sources in an urban region. – Journal of Geophysical Research 115: 1-13.

[3] Fang, S., Tans, P. P., Yao, B., Luan, T., Wu, Y., Yu, D. (2017): Study of atmospheric CO_2 and CH_4 at Longfengshan WMO/GAW regional station: the variations, trends, influence of local sources/sinks, and transport. – Science China Earth Sciences 60: 1886-1895.

[4] Feng, Y., Bie, P., Wang, Z., Wang, L., Zhang, J. (2017): Bottom-up anthropogenic dichloromethane emission estimates from China for the period 2005-2016 and predictions of future emissions. – Atmospheric Environment 186: 241-247. https://doi.org/10.1016/j.atmosenv.2018.05.039.

[5] Gamnitzer, U., Karstens, U., Kromer, B., Neubert, R. E. M., Meijer, H. A. J., Schroeder, H., Levin, I. (2006): Carbon monoxide: a quantitative tracer for fossil fuel CO_2? – Journal of Geophysical Research 111.

[6] Gilliland, A. B., (2003): Seasonal NH_3 emission estimates for the eastern United States based on ammonium wet concentrations and an inverse modeling method. – Journal of Geophysical Research 108.

[7] Hu, C., Liu, S., Wang, Y., Zhang, M., Xiao, W., Wang, W., Xu, J. (2018): Anthropogenic CO_2 emissions from a megacity in the Yangtze River Delta of China. – Environmental Science and Pollution Research 25: 23157-23169.

[8] Levin, I., Hesshaimer (2000): Radiocarbon - A Unique Tracer of Global Carbon Cycle Dynamics. – In: Tull, A. J. T. (ed.) Radiocarbon. Cambridge University Press, Cambridge, pp. 69-80.

[9] Levin, I., Karstens, U. (2007): Inferring high-resolution fossil fuel CO_2 records at continental sites from combined $^{14}CO_2$ and CO observations. – Tellus 59B: 245-250

[10] Levin, I., Karstens, U. (2008): Quantifying Fossil Fuel CO 2 over Europe. – In: Dolman, A. J., Valentini, R., Freibauer, A. (eds.) The Continental-Scale Greenhouse Gas Balance of Europe. Ecological Studies, Vol. 203. Springer, New York,

[11] Levin, I., Kromer, B. (2004): The tropospheric $^{14}CO_2$ level in mid-latitudes of the northern hemisphere (1959-2003). – Radiocarbon 46: 1261-1272.

[12] Levin, I., Kromer, B., Schmidt, M., Sartorius, H. (2003): A novel approach for independent budgeting of fossil fuel CO_2 over Europe by $^{14}CO_2$ observations. – Geophysical Research Letters 30.

[13] Li, M., Zhang, Q., Kurokawa, J. I., Woo, J. H., He, K., Lu, Z., Ohara, T., Song, Y., D. Streets, G., Carmichael, G. R., Cheng, Y., Hong, C., Huo, H., Jiang, X., Kang, S., Liu, F., Su, H., Zheng, B. (2017): MIX: a mosaic Asian anthropogenic emission inventory under the international collaboration framework of the MICS-Asia and HTAP. – Atmos. Chem. Phys. 17: 935-963.

[14] Li, M., Zhang, Q., Kurokawa, J., Woo, J. H., He, K. B., Lu, Z., Ohara, T., Song, Y., Streets, D. G., Carmichael, G. R., Cheng, Y. F., Hong, C. P., Huo, H., Jiang, X. J., Kang, S. C., Liu, F., Su, H., Zheng, B. (2015): MIX: a mosaic Asian anthropogenic emission

http://www.aloki.hu ● ISSN 1589 1623 (Print) ● ISSN 1785 0037 (Online)
DOI: http://dx.doi.org/10.15666/aeer/2206_53115327

inventory for the MICS-Asia and the HTAP projects. – Atmospheric Chemistry and Physics Discussions 15: 34813-34869.
[15] Lu, L., Chen, B., Guo, L. (2019): A regional data assimilation system for estimating CO surface flux from atmospheric mixing ratio observations—a case study of Xuzhou, China. – Environ Sci Pollut Res 2019: 8748-8757.
[16] Meijer, H., Smid, H. M., Keizer, M. G. (1996): Isotopic Characterisation of Anthropogenic CO_2 Emissions Using Isotopic and Radiocarbon Analysis. – Physics and Chemistry of the Earth 21: 483-487.
[17] Mottungan, K., Brocchi, V., Roychoudhury, C., Gaubert, B., Tang, W., Mirrezaei, M. A., McKinnon, J., Guo, Y., Avelino, A. (2024): Local and regional enhancements of CH_4, CO, and CO_2 inferred from TCCON column measurements. – EGUsphere. https://doi.org/10.5194/egusphere-2024-705 (in print).
[18] Ohara, T., Akimoto, H., Kurukawa, J., Horii, N. 2007, An Asian emission inventory of anthropogenic emission sources for the period 1980-2020. – Atmos. Chem. Phys. 4419-4444.
[19] Palmer, P. I., Suntharalingam, P., Jones, D., Jacob, D. J., Streets, D. G. (2006): Using CO_2:CO correlations to improve inverse analyses of carbon fluxes. – Journal of Geophysical Research: Atmospheres 111. https://doi.org/10.1029/2005JD006697.
[20] Potosnak, M. J., Wofsy, S. C., Denning, A. S., Conway, T. J., Munger, J. W., Barnes, D. H. (1999): Influence of biotic exchange and combustion sources on atmospheric CO_2 concentrations in New England from observations at a forest flux tower. – Journal of Geophysical Research: Atmospheres 104: 9561-9569.
[21] Rivier, L., Ciais, P., Hauglustaine, D. A., Bakwin, P., Bousquet, P., Peylin, P., Klonecki, A. (2006): Evaluation of SF_6, C_2Cl_4, and CO to approximate fossil fuel CO_2 in the Northern Hemisphere using a chemistry transport model. – Journal of Geophysical Research 111.
[22] Sahu, S. K., Beig, G., Parkhi, N. (2015): High resolution emission inventory of NO_x and CO for mega city Delhi, India. – Aerosol and Air Quality Research 15: 1137-1144.
[23] Shan, W., Zhou, H., Mao, J., Ding, Q., Cui, Y., Zhao, F., Xiong, C., Li, H. (2023): Effect of combustion conditions and blending ratio on aero-engine emissions. – Energies 16: 7060.
[24] Suntharalingam, P., Jacob, D. J., Palmer, P. I., Logan, J. A., Yantosca, R. M. (2004): Improved quantification of Chinese carbon fluxes using CO_2/CO correlations in Asian outflow. – Journal of Geophysical Research 109.
[25] Svetlik, I., Povinec, P. P., Molnár, M., Meinhardt, F., Michálek, Simon, J., Svingor, É. (2010): Estimation of long-term trends in the tropospheric $^{14}CO_2$ activity concentration. – Radiocarbon 52: 815-822.
[26] Turnbull, J. C., Miller, J. B., Lehman, S. J., Tans, P. P., Sparks, R. J., Southon, J. (2006): Comparison of $^{14}CO_2$, CO, and SF_6 as tracers for recently added fossil fuel CO_2 in the atmosphere and implications for biological CO_2 exchange. – Geophysical Research Letters 33.
[27] Vogel, F., Hamme, S., Steinhof, A., Kromer, B., Levin, I. (2017): Implication of weekly and diurnal ^{14}C calibration on hourly estimates of CO-based fossil fuel CO_2 at a moderately polluted site in southwestern Germany. – Tellus B: Chemical and Physical Meteorology 62: 512-520.
[28] Yue, T., Zhang, L., Zhao, M., Wang, Y., Wilson, J. (2016): Space-and ground-based CO_2 measurements: a review. – Science China Earth Sciences 59: 2089-2097.
[29] Zhao, J., Chen, H., Qi, X., Chi, X., Jia, M., Jiang, F., Zhong, S., Zheng, B., Ding, A. (2024): Observed decade-long improvement of combustion efficiency in the Yangtze River Delta region in China. – Environmental Research Letters 19.
[30] Zou, M., Chen, L., Li, S., Fan, M., Tao, J., Zhang, Y. (2017): An improved constraint method in optimal estimation of CO_2 from GOSAT SWIR observations. – Science China Earth Sciences 60: 286-296.